Published in final edited form as:
Bone. 2009 February ; 44(2): 287–294. doi:10.1016/j.bone.2008.10.040.

Molecular Analysis of DMP1 Mutants Causing Autosomal Recessive Hypophosphatemic Rickets

Emily G. Farrow[1], **Siobhan I. Davis**[1], **Leanne M. Ward**[2], **Lelia J. Summers**[1], **Judith S. Bubbear**[3], **Richard Keen**[3], **Trevor C.B. Stamp**[3,4], **Laurence R. I. Baker**[5], **Lynda F. Bonewald**[6], and **Kenneth E. White**[1]

1 *Department of Medical & Molecular Genetics, Indiana Univ. School of Medicine, Indianapolis, IN, USA*

2 *Department of Pediatrics, Children's Hospital of Eastern Ontario, and the University of Ottawa, Ottawa, Ontario, Canada*

3 *Metabolic Unit, Royal National Orthopaedic Hospital, Stanmore, Middlesex, UK*

4 *UCL Hospital, London UK*

5 *Department of Nephrology, St. Bartholomew's and Royal London Hospitals, London UK*

6 *Department of Oral Biology, University of Missouri-Kansas City, Kansas City, MO, USA*

Abstract

We previously demonstrated that the mutations Met1Val (M1V) and the deletion of nucleotides 1484-1490 (1484-1490del) in Dentin matrix protein-1 (DMP1) cause the novel disorder autosomal recessive hypophosphatemic rickets (ARHR), which is associated with elevated Fibroblast growth factor-23 (FGF23). To further understand the role of DMP1 in ARHR, we undertook molecular genetic and in vitro expression studies. First, we examined a kindred with a severe hypophosphatemic rickets phenotype and recessive inheritance. Analyses of this family demonstrated that the affected members had elevated serum FGF23 and carried a large, biallelic deletion that removed the majority of *DMP1*. At a minimum, this deletion encompassed 49 kb between *DMP1* exon 3 and an intergenic region 5′ to the next telomeric gene, integrin-binding sialoprotein (IBSP). We next performed immunofluorescent studies in cells to understand the effects of the known ARHR mutations on DMP1 cellular processing. These analyses showed that the M1V DMP1 mutant was not sorted to the trans-Golgi network (TGN) and secretory pathway, but filled the entire cytoplasm. In contrast, the 1484-1490del mutant localized to the TGN and was secreted, similar to wild type DMP1. The 1484-1490del mutation replaces the DMP1 18 C-terminal amino acids with 33 non-native residues. Truncation of wild type DMP1 by these native 18 residues followed by Western blot and confocal microscopic analyses demonstrated a wild type expression pattern when compared with the 1484-1490del mutant, indicating that the last 18 residues are not critical for cellular trafficking, but that the 33 additional residues arising from the 1484-1490del mutation likely compromise DMP1 processing. The relationship between DMP1 and FGF23 is unclear. To test endogenous DMP1 response to serum metabolites that also regulate FGF23, UMR-106 cells were treated with 1,25 $(OH)_2$ vitamin D (1×10^{-7}M) and showed a 12-fold increase in DMP1 mRNA and protein at 24 hr.

Corresponding author information: Kenneth E. White, Ph.D., Department of Medical & Molecular Genetics, Indiana University School of Medicine, 975 West Walnut St., IB130, Indianapolis, IN 46202, Office phone: (317) 278-1775, Fax: (317) 274-2293, E-mail: kenewhit@iupui.edu.

In summary, we have identified a novel DMP1 deletion as the cause of ARHR, as well as demonstrated that the ARHR mutations alter DMP1 cellular processing, and that DMP1 can be regulated by vitamin D. Taken together, this work expands our understanding of the genetic and molecular mechanisms associated with DMP1 alterations causing ARHR.

Keywords

FGF23; vitamin D; ARHR; SIBLING; hypophosphatemia

INTRODUCTION

Isolated renal phosphate wasting and subsequent hypophosphatemia may result from a number of genetic syndromes that include: autosomal dominant hypophosphatemic rickets (ADHR), X-linked hypophosphatemic rickets (XLH), and autosomal recessive hypophosphatemic rickets (ARHR). ARHR (OMIM #241520) is characterized by a similar biochemical phenotype to that of ADHR and XLH, including elevated serum Fibroblast growth factor-23 (FGF23) and inappropriately normal $1,25(OH)_2$ vitamin D concentrations in most patients [1]. Furthermore, ARHR patients manifest peri-osteocytic lesions upon bone biopsy, which are a hallmark of XLH [1]. We previously demonstrated that homozygous mutations in Dentin matrix protein-1 (*DMP1*), including the deletion of nucleotides 1484-1490 (1484-1490del) and the missense replacement of the initial methionine with valine, (Met1Val, or 'M1V' mutant), are causative for ARHR [1]. Other investigators similarly identified the DMP1 M1V mutation [2], as well as splice-site mutations in the DMP1 gene in consanguineous kindreds [2]. Taken together with the hypophosphatemic rickets phenotype of the *Dmp1*-null mouse, these findings indicate that loss of DMP1 function results in ARHR.

DMP1 is a member of the 'SIBLING' (Small Integrin Binding Ligand N-linked Glycoprotein) family, which is a group of non-collagenous extracellular matrix proteins involved in bone mineralization [3]. These genes are localized to human chromosome 4q21–25 [3], have similar exon arrangements, and include dentin sialoprotein (DSP), dentin phosphoprotein (DPP), osteopontin (OPN), integrin-binding sialoprotein (IBSP), and matrix extracellular phosphoglycoprotein (MEPE) [3].

The SIBLING proteins share common structural features, such as multiple phosphorylation sites, a highly acidic nature, the presence of an arginine-glycine-aspartic acid (RGD) cell attachment domain, and proteolytic-resistant acidic serine-aspartate-rich MEPE-associated motif (ASARM motif) [3,4]. DMP1 is highly expressed in osteocytes and is comprised of 513 residues, but is secreted in bone and dentin as 37 kD N-terminal (residues 17–253), and 57 kD C-terminal (residues 254–513) fragments from a 94 kD full-length precursor. Recombinant DMP1 binds calcium-phosphate ions [5] and the N-telopeptide region of type 1 collagen [6] with high affinities. Potential roles for DMP1 in bone and teeth may include regulating hydroxyapatite formation [7], and depending upon proteolytic processing and phosphorylation [8], may regulate local mineralization processes in vivo [7].

The molecular consequences of the ARHR alterations on DMP1 expression are unknown. Therefore, we undertook studies to further understand ARHR through genetic analyses of a kindred with hypophosphatemia and recessive inheritance, and by testing the cellular processing of the known ARHR mutants M1V and 1484-1490del.

MATERIALS AND METHODS

ARHR patients

All subjects provided written, informed consent in accord with the Institutional Review Board of Indiana University and the Royal London Hospitals, London UK. Routine serum biochemistries were assessed using standard protocols. Intact FGF23 serum concentrations were determined using an ELISA according to the manufacturer's protocol (Kainos Laboratories International; Tokyo, Japan). This assay utilizes monoclonal antibodies and has been shown to recognize full-length human FGF23 [9]. C-terminal FGF23 levels were also determined by ELISA (Immutopics Inc.; San Clemente, CA). This assay utilizes polyclonal antibodies and has been shown to recognize both full-length and C-terminal fragments of human FGF23 [10].

DMP1 mutation detection

Genomic DNA was extracted from blood samples using the Qiamp DNA Blood Extraction kit (Qiagen, Inc.; Valencia, CA) according to the manufacturer's protocol. DMP1 exons were PCR-amplified as described previously [1] with intronic primers (available upon request) using 20 ng of genomic DNA as template. Primers were also designed to the first exon of Integrin-binding sialoprotein (IBSP), the gene immediately telomeric to DMP1. PCR conditions for all experiments were: 1 min 95°C, followed by 35 cycles of 30 seconds 95°C, 30 seconds 57°C, 1 min 72°C, and a final extension of 7 min at 72°C. Amplified exons were resolved on 1.5% agarose gel stained with ethidium bromide.

ARHR mutant plasmids and truncation of DMP1

The 1480–1490del and M1V ARHR mutants were generated from a human DMP1 cDNA in pcDNA3.1(+)V5-His as previously described [1]. To truncate DMP1 for the 18 wild type residues (plasmid 'DMP1Δ18') removed by the 1484-1490del mutation, the native DMP1 plasmid was amplified with *PfU* polymerase (Stratagene) using a forward primer encompassing the initial methionine (5′-tggagagaaacatctatgtcc-3′) and an internal reverse primer (5′-gcagaattctgcatcaactgttaatt-3′). PCR conditions were: 1 min 95°C, followed by 35 cycles of 30 s 95°C, 50 s 60°C, 1 min 68°C, and a final extension of 7 min at 68°C. The truncated cDNA was cloned into pcDNA3.1(+)V5-His using standard protocols. To make untagged constructs, plasmids for wild type DMP1 and each mutant had a stop codon introduced 5′ to the V5-His tag in pcDNA3.1(+)V5-His using the Quickchange Site-directed Mutagenesis Kit (Stratagene, Inc.) according to the manufacturer's instructions. The primers for each plasmid were as follows: M1V and wild type DMP1: forward: 5′-gactgccaagacggctattaattctgcagatatccag-3′, reverse: 5′-ctggatatctgcagaattaatagccgtcttggcagtc-3′; and the 1484-1490del DMP1: forward: 5′-taaaggagtcttagggacttaattctgcagatatccagc-3′, reverse: 5′-gctggatatctggagaattaagtccctaagactccttta-3′ (stop codons underlined). All plasmids were sequenced to confirm mutation of the targeted residues and maintenance of the ORF.

Cell culture

UMR-106 and HEK293 cells (American Type Culture Collection) were cultured in D-MEM/F-12 (Invitrogen) supplemented with 10% fetal bovine serum (FBS) (Hyclone), 1 mM sodium pyruvate, 25 mM L-glutamine, and 25 mM penicillin-streptomycin at 37°C and 5% CO_2. MC3T3 cells were cultured in α-MEM/F-12 (Invitrogen) supplemented with 10% FBS, 1mM sodium pyruvate, 25mM L-glutamine, and 25 mM penicillin-streptomycin at 37°C and 5% CO_2. Cells were sub-cultured every 3 days. For transfection, cells were seeded on 60 mm plates. After 24 h the cells were transfected with 2 μg of plasmid DNA in supplemented D-MEM/F-12 or α-MEM/F-12 lacking fetal bovine serum, using either Fugene 6 (Roche) transfection

reagent (UMR-106 and HEK293) or Lipofectamine (Invitrogen) (for MC3T3) following manufacturer's protocol.

Western analyses

Conditioned media was collected from DMP1-transfected cells, and the cells were washed three times with 1X PBS, and then lysed with 0.125 ml 1X Lysis Buffer (Cell Signaling Technologies; Danvers, MA) in the presence of the protease inhibitor AEBSF (10 μg/mL). Conditioned media and cellular lysate samples were combined 1:1 with Laemmli Sample Buffer (Bio-Rad) and boiled for 5 min. Samples were electrophoresed on 15% SDS-PAGE mini-gels (Bio-Rad) and electrotransferred to PVDF membranes (Bio-Rad) for 2.5 hours. Membranes were blocked with 5% Blotto (Carnation non-fat dry milk in 1X PBS) with shaking overnight at 4°C. Membranes were incubated with primary antibody (anti-V5 conjugated to HRP, Invitrogen, Inc.; anti-human DMP1 LF148 [11,12], a generous gift from Dr. Larry Fisher, NIH; or an affinity-purified rabbit polyclonal antibody to rodent Dmp1 (anti-Dmp1 #784)) for 2 h, then washed three times with 1X TBS with 0.05% Tween 20. Membranes were incubated with 1:3000 secondary antibody anti-rabbit HRP for 1 hr, then washed three times with 1X TBS with 0.05% Tween 20. Visualization was performed using the ECL Plus Western Blotting Detection Reagents (Amersham GE Healthcare).

Immunofluorescence

All cell lines (UMR-106, HEK293, MC3T3) were seeded (1×10^4) in 4-well chamber slides (Nalge Nunc International). After 24 h, cells were transfected with either wild type or the DMP1 mutant plasmids using either the Fugene 6 (Roche) transfection reagent (for HEK293 and UMR-106) or Lipofectamine (Invitrogen) (for MC3T3). The cells were incubated for an additional 24 h and then fixed with 4% paraformaldehyde for 15 min, permeabilized in 1X PBS with 0.1% Igepal (Sigma) for 30 min, and blocked with 1X PBS with 3% BSA (Invitrogen) and 0.1% Igepal at 37°C for 1 h. The cells were probed with either anti-V5, an anti-human DMP1 antibody (LF148), or anti-TGN38 (Sigma) for 1 h at 37°C, followed by three washes with 1X PBS with 0.1% Igepal, and probed with the appropriate secondary fluorescent antibodies. Wheat Germ Agglutinin (WGA)-Texas Red (Molecular Probes) was also used to stain the trans-Golgi network (TGN). The chambers were removed from the slide, and Vectashield mounting media with DAPI (Vector Laboratories) was added with a cover slip prior to visualization. Imaging was performed using a Zeiss UV LSM-510 confocal microscope (Carl Zeiss, Inc. Thornwood, NY) and a Leica DM5000B fluorescent microscope (Leica Microsystems, Inc). Images were captured using the Zeiss LSM-510 software (Carl Zeiss, Inc. Thornwood, NY) and a SPOT camera and computer program (RTKE Diagnostic Instruments, Inc).

Quantitative RT-PCR (qPCR)

UMR-106 cells were treated with 1×10^{-7}M $1,25(OH)_2$ vitamin D and the RNA was harvested from the cellular lysates using the RNeasy kit (Qiagen, Inc.). RNA samples were tested with intron-spanning primers specific for rat DMP1 mRNA (forward 5′-ggctgtcctgtgctctccc-3′, reverse 5′-ttgcccgtccgctcttc-3′, probe 5′-gcggagataccaaaatactgaatctgaaa gctc-3′), rat FGF23 (forward 5′-cggcaacatttttggatcgt-3′, reverse 5′-agcgtccactggcgga-3′, probe 5′-tcacttcagcccggagaactgcaga-3′), and rodent GAPDH (Applied Biosystems) was used as an internal control. The TaqMan One-Step RT-PCR kit was used to perform qPCR. PCR conditions for all experiments were: 30 min 48°C, 10 min 95°C, followed by 40 cycles of 15 sec 95°C and 1 min 60°C. The data was collected and analyzed by the 7500 Real Time PCR system and software (Applied Biosystems). At each time point, the expression levels of DMP1, FGF23, and GAPDH mRNAs were calculated relative to vehicle-only treated UMR-106 cells. All primer sets were tested for specific amplification of mRNA by parallel analyses of controls

that included omitting RT or template, and resulted in no fluorescent signal detection. Each RNA sample was analyzed in triplicate, and each experiment was performed independently at least three times. The $2^{-\Delta\Delta CT}$ method described by Livak was used to analyze the data [13].

RT-PCR

UMR-106 cells were treated with either vehicle or 1×10^{-7}M $1,25(OH)_2$ vitamin D and the RNA harvested from the cellular lysates using the RNeasy kit (Qiagen, Inc.). Following reverse transcription (RT), RNA samples were tested with intron-spanning primers specific for rat FGF23 mRNA (crossing the 4900 bp FGF23 intron 1: forward 5′-ccatagggatggccatgtag-3′, reverse 5′-tgatgcttcggtgacaggta-3′). The GeneAmp kit (Applied Biosystems) was used to perform RT-PCR: RT conditions were 10 min 25°C, 25 min 42°C, 5 min 95°C, and 5 min 4°C; PCR conditions were 2 min 95°C, followed by 35 cycles of 1 min 95°C, 1 min 57°C, and 1 min 72°C, followed by 7 min of 72°C.

Statistical analysis—Statistical analysis of the data was performed by Student's t-test and significance for all tests was set at $P<0.05$. Data are presented as means ± standard error of the mean (SEM).

RESULTS

Genetic analyses of an ARHR kindred

To further understand the role of DMP1 in ARHR, we assessed a family previously characterized as having hypophosphatemic rickets [14]. The parents of the affected individuals are known to be first cousins, therefore autosomal recessive inheritance was presumed upon evaluation of parental blood types. Subsequently paternity was confirmed by HLA/DR markers and genetic fingerprinting [15]. The patients, an affected brother and sister, individuals II-1 and II-3, respectively (Figure 1), both presented with rickets as children. These individuals have a severe disease course manifested by marked hypophosphatemia, persistent osteomalacia upon bone biopsy, increased bone density by dual-energy X-ray absorptiometry, stunted growth, nerve deafness, facial and dental abnormalities, and learning disabilities [14].

Blood samples were available from the father and both affected siblings for biochemical and genetic evaluations. The patients' current laboratory biochemistries are listed in Table 1. The father (individual I-1) was previously assessed as normophosphatemic [14]. Intact serum FGF23 for the father was 42.33 pg/mL (normal range 10–54 pg/mL), whereas the patients' values were elevated at 91.5 pg/mL (patient II-1) and 199 pg/mL (patient II-3). In correlation with the intact serum values, the C-terminal serum FGF23 value for the father (II-1) was 80 Reference Units (RU)/mL (normal range 10–150 RU/mL), whereas the patients' levels were elevated at 441 RU/mL (patient II-1) and 525 RU/mL (patient II-3). It is noteworthy that the FGF23 values were obtained while patient II-1 was receiving a therapeutic regimen of 0.75 mcg of calcitriol and 1.25 g of chewable calcium carbonate per day, and patient II-3 received 0.75 mcg calcitriol daily.

Given the patients' documented history of hypophosphatemic rickets with recessive inheritance and that Dentin matrix protein-1 (DMP1) has previously been associated with autosomal recessive hypophosphatemic rickets (ARHR), sequencing for *DMP1* mutations was undertaken. Following PCR targeting of the genomic DNA comprising DMP1, these analyses revealed no PCR products for *DMP1* exons 3 through 6 in the affected individuals, but a normal PCR pattern in the father (Figure 1A). The integrin-binding sialoprotein (*IBSP*) gene, another SIBLING family member, is located telomeric to DMP1. As determined by PCR, an intronic DNA sequence approximately 49 kb telomeric to the DMP1 stop codon and 96 kb centromeric to exon 1 of the IBSP gene, was also deleted in the affecteds but not in the parent (Figure 1A).

However, the first exon of IBSP was intact in both patients and in the father, thus the size of deletion is at least 49 kb (from DMP1 exon 3 to the intronic sequence between DMP1 and IBSP), and maximally 145 kb (from DMP1 exon 3 to the first exon of IBSP; summarized in Figure 1B).

Due to the recessive inheritance in this kindred [14,15], taken together with the fact that we found no other mutations in the father's DMP1 sequences, we assume that the father is a carrier for the large deletion (mother was not available for analyses) and that the DMP1 PCR products arising from his genomic DNA sample (Figure 1A) are from the single copy of the normal allele. The presence of PCR products from the 5′ portions of DMP1 (exon 2) and from a 5′ region IBSP (exon 1), coupled with the lack of DMP1 PCR products from intervening sequences that are known to amplify genomic DNA of normal individuals [1] and in the father (Figure 1A), indicate that the recessive hypophosphatemia in these patients is due to loss of most of the DMP1 gene through a large, 3′ deletion.

Effects of ARHR DMP1 mutations on subcellular localization

We previously identified two mutations in *DMP1* that result in ARHR, the first was a homozygous 7 base pair deletion in exon 6 (1484-1490del), resulting in the replacement of the last 18 highly conserved amino acids with 33 novel residues [1]. The second mutation was a homozygous A to G transition at position 1 leading to the replacement of the initial methionine with valine (M1V), which would potentially compromise the DMP1 signal sequence [1]. The effect of the ARHR mutations on the intracellular processing of DMP1 are unknown, therefore we performed confocal immunolocalization studies in UMR-106, HEK293, and MC3T3 cells following transfection of wild type and the ARHR DMP1 mutants. Consistent with their secretion into the media, wild type and 1484-1490del DMP1 were found to co-localize with the TGN using an antibody to the C-terminal V5 tag carried on these proteins. In stark contrast, the M1V mutant did not co-localize with the TGN, but rather filled the entire cytoplasm, likely having altered cellular sorting due to loss of the signal peptide (Figure 2A). These results were confirmed in UMR-106 cells using an antibody specific for a TGN marker (protein TGN38) (Figure 2B). Due to the apparent importance of the DMP1 C-terminus as implicated by the ARHR 1484-1490del mutation, and to assure that the V5 tag did not interfere with cellular sorting, we repeated the experiments with wild type and ARHR-mutant plasmids carrying a stop codon upstream of the V5-His tag. Using the untagged plasmids and an anti-human DMP1 antibody, LF148 [11,12], we obtained the same results in all cell lines, with the wild type and deletion mutants co-localizing with the TGN, and the M1V mutant filling the cell cytoplasm (Figure 2C).

Functional analysis of the DMP1 C-terminal tail

To compare the cellular processing of the ARHR-mutant isoforms with wild type DMP1, the M1V, and 1484-1490del mutants were transiently transfected into HEK293 cells for Western blot analysis (Figure 3). In agreement with our previous results [1], wild type DMP1 was detected in the media as an intact, 94 kD species as well as a well-characterized 57 kD proteolytically cleaved 3′ species. In contrast, the 1484-1490del mutant was primarily detected as the 57 kD cleavage product, with reduced presence of the 94 kD species in the media (n=6).

To test the function of the highly conserved DMP1 C-terminal tail and compare expression with the known DMP1 mutants, the last 18 amino acids replaced in the frameshift caused by the 1484-1490del mutation were removed from the DMP1 cDNA to develop the DMP1Δ18 plasmid. When compared to the 1484-1490del mutant, Western blotting indicated that DMP1Δ18 reverted back to the wild type DMP1 distribution in the media, with a balanced expression of the 94 and 57 kD products (Figure 3A). These results indicated that the altered processing of the 1484-1490del mutant in the conditioned media (i.e. reduced expression of

the 94 kD band) is not simply due to the loss of the last 18 amino acids, but to an affect of gaining the additional 33 non-native residues. Furthermore, analysis of the DMP1Δ18 by confocal immunofluorescence in HEK293 cells showed co-localization of the truncated DMP1 with the TGN (Figure 3B), supporting the results from the Western analyses in Figure 3A, which demonstrated proper secretion of the truncated DMP1.

Regulated DMP1 expression in UMR-106 cells

The loss of DMP1 in ARHR results in the up-regulation of FGF23 in osteocytes [1], however the relationship between FGF23 and DMP1 is unclear. To begin to understand potentially coordinated expression of DMP1 and FGF23, we investigated whether DMP1 expression was controlled by metabolites that also affect FGF23 production. It was previously shown that treatment of UMR-106 cells with $1,25(OH)_2$ vitamin D results in increased FGF23 mRNA [16]. To test expression of DMP1, UMR-106 cells were treated with 1×10^{-7}M $1,25(OH)_2$ vitamin D (1,25D) for 8 and 24 hours. Analyses by qPCR revealed a 2-fold increase in DMP1 mRNA at 8 h, and a 12-fold increase at 24 h in the 1,25D-treated cells when compared to control (Figure 4A) ($P<0.05$). Consistent with these results, an increase in DMP1 protein was detected in the 1,25D treated cells as assessed by Western analysis (Figure 4A, *Inset*). FGF23 also demonstrated a significant increase in mRNA expression, as assessed by qPCR and RT-PCR over the same time course (Figures 4B and 4C), indicating that both DMP1 and FGF23 are responsive to vitamin D.

In summary, we identified a new DMP1 mutation that leads to ARHR, have shown biological differences in the cellular sorting of known ARHR DMP1 mutants, as well as determined that the novel residues that arise in the ARHR DMP1 1484-1490del mutant likely compromise this polypeptide. Finally, DMP1 and FGF23 are concordantly regulated by vitamin D in vitro.

DISCUSSION

ARHR is due to inactivating mutations in *DMP1*, however the molecular mechanisms in bone cells underlying the manifestations of this syndrome are unknown. We identified a novel deletion in the DMP1 gene as the cause of ARHR in a family with a confirmed recessive inheritance pattern (Figure 1). Previously-characterized ARHR patients have been found to have alterations in the *DMP1* start codon (M1V) and in the C-terminal domain (exon 6) [1,2], as well as splice-site mutations in the 5′ portions of the gene that would result in markedly truncated protein products [2]. The identification herein of a large deletion in ARHR confirms the role of DMP1 in this disease, and widens the spectrum of molecular defects that result in this disorder. Of note, our patients appear to have a more severe phenotype than those with the previously reported DMP1 mutations [2,17]. The *IBSP* gene, the next gene telomeric to DMP1 also encodes a SIBLING protein, which is expressed in hypertrophic chondrocytes, osteoblasts, osteocytes, and osteoclasts [18]. Although the first exon of IBSP was intact in both affected patients in this study, it is possible the deletion affects the upstream regions of *IBSP*, and that this family may represent a contiguous gene syndrome. Given the apparent rarity of ARHR, the variable expressivity in this disorder, as well as the similarities between *Hyp* and *Dmp1*-null mice, however, the phenotype observed in this family could be solely due to the *DMP1* deletion, and represent a manifestation of similar clinical and biochemical findings as observed in some severe cases of XLH [19–21]. Furthermore, the *Ibsp* gene has not been deleted in mice, therefore it is difficult at this time to distinguish in vivo the phenotypes that may be solely due to the loss of *DMP1* and the phenotypes that would only be due to loss of *IBSP*.

DMP1 is an extracellular matrix protein known to be secreted into mineralizing bone and dentin [22], however the cellular sorting and trafficking of the DMP1 ARHR mutants is unknown. We previously demonstrated that in vitro, wild type DMP1 is expressed equally in cellular lysates and the conditioned media, the 1484-1490del mutant is primarily detected in the media,

and the M1V mutant is wholly retained within the cell lysate [1]. In the present work, analyses of the subcellular localization of DMP1 by confocal microscopy revealed that both wild type, 1484-1490del DMP1, and a truncated DMP1Δ18 isoform localize to the TGN, consistent with these proteins acting as secreted entities in the mineralizing bone matrix [23]. In contrast, our analyses showed that the M1V mutant does not enter into the TGN and fills the entire cytoplasm, most likely due to the loss of the signal sequence (Figure 2). Consistent with our results, native Dmp1 has previously been detected in MC3T3 cells in both the intracellular compartments and in the extracellular milieu [22].

DMP1 can be found in bone as a full-length, 94 kD species, as well as N-terminal 37 kD fragments and C-terminal 57 kD fragments. The function of the N-terminal portion of DMP1 is largely unknown, however the C-terminal portion of DMP1 has been previously implicated as having roles in DNA binding and gene regulation [24], bone mineralization and potentially cross-linking with collagen [7], and as an integrin-binding protein [3]. How these functions are related to the processing of DMP1 and its role in aberrant osteocyte differentiation in ARHR [1,2], however, remain to be determined. Before we and others discovered the ARHR mutations, the highly conserved 18-residue DMP1 tail altered by the 1484-1490del mutation was unexplored with regard to biological importance in function or in protein stability. In the present work, when human DMP1 was truncated by the last 18 residues, the expression was similar to wild type protein, with balanced production of the 94 and 57 kD protein species in the conditioned media (Figure 3A). These results indicate that the last 18 amino acids, although highly conserved across species, are not critical for DMP1 expression. Therefore, in the case of the 1484-1490del mutant, aberrant protein expression may not be due to the loss of the last 18 amino acids, but is most likely a function of adding the 33 novel amino acids to the C-terminus of DMP1. Whether the additional residues compromise DMP1 folding or interfere with the overall charge of the mature molecule is unknown at this time. It is clear however, that when DMP1 is not secreted (M1V mutation), or is secreted but carries a 3′ mutation (1484-1490del), or deleted (Figure 1A), ARHR patients manifest hypophosphatemic bone disease.

The loss of *DMP1*/*Dmp1* results in a hypophosphatemic rickets phenotype associated with elevated FGF23 that parallels the disease courses of XLH and ADHR. However the molecular mechanisms underlying the regulation of DMP1 at the transcriptional level, and how the reduced or altered expression of this gene affects FGF23 expression is not clear. We have shown that native Dmp1 expressed in UMR-106 cells is responsive to treatment with vitamin D (Figure 4), indicating that Dmp1 is regulated by metabolites that are known to increase FGF23 mRNA production [25,26]. It has also previously been shown that Dmp1 mRNA expression in differentiating murine cementoblasts is upregulated in response to treatment with phosphate [17], a metabolite which may also regulate FGF23 in mouse [27] and in humans [28,29]. It is tempting to speculate that because FGF23 is upregulated in ARHR, that lack of DMP1 results in a direct effect of increased FGF23 expression, and that under normal circumstances, DMP1 is stimulated by vitamin D to repress elevated FGF23 as part of a negative feedback loop. In ARHR, however, as shown in the *Dmp1*-null mouse, the primary cellular defect may be an alteration in osteoblast to osteocyte maturation, leading to inappropriate expression of typically ‘osteoblastic’ or ‘early osteocyte’ genes such as type I collagen, alkaline phosphatase, and FGF23, in mature embedded osteocytes [1]. As opposed to direct effects on FGF23, the hormonal control of DMP1 may provide a novel avenue instead, for understanding regulated FGF23 expression as bone cells undergo differentiation.

In summary, we have identified a novel deletion in the *DMP1* gene that results in ARHR with a severe phenotype, and have shown that the ARHR DMP1 mutants are either mis-sorted in bone cells or altered due to mutations in the N- and C-terminal portions of the molecule,

respectively. Finally, in vitro, *Dmp1* is responsive to vitamin D, a metabolite that also increases FGF23 production.

Acknowledgements

The authors would like to acknowledge the participation of all patients, as well as NIH grants DK063934 (KEW) and AR046798 (LFB); an IUPUI Graduate Student Fellowship (EGF); Canadian Institutes for Health Research New Investigator Program and the Canadian Child Health Clinician Scientist Program (LMW); the Indiana Center for Biological Microscopy; and the Indiana Genomics Initiative (INGEN) of Indiana University, supported in part by the Lilly Endowment, Inc. (KEW).

References Cited

1. Feng JQ, Ward LM, Liu S, Lu Y, Xie Y, Yuan B, Yu X, Rauch F, Davis SI, Zhang S, Rios H, Drezner MK, Quarles LD, Bonewald LF, White KE. Loss of DMP1 causes rickets and osteomalacia and identifies a role for osteocytes in mineral metabolism. Nat Genet 2006;38:1310–5. [PubMed: 17033621]
2. Lorenz-Depiereux B, Bastepe M, Benet-Pages A, Amyere M, Wagenstaller J, Muller-Barth U, Badenhoop K, Kaiser SM, Rittmaster RS, Shlossberg AH, Olivares JL, Loris C, Ramos FJ, Glorieux F, Vikkula M, Juppner H, Strom TM. DMP1 mutations in autosomal recessive hypophosphatemia implicate a bone matrix protein in the regulation of phosphate homeostasis. Nat Genet 2006;38:1248–50. [PubMed: 17033625]
3. Fisher LW, Fedarko NS. Six genes expressed in bones and teeth encode the current members of the SIBLING family of proteins. Connect Tissue Res 2003;44(Suppl 1):33–40. [PubMed: 12952171]
4. Butler WT, Ritchie H. The nature and functional significance of dentin extracellular matrix proteins. Int J Dev Biol 1995;39:169–79. [PubMed: 7626404]
5. He G, Gajjeraman S, Schultz D, Cookson D, Qin C, Butler WT, Hao J, George A. Spatially and temporally controlled biomineralization is facilitated by interaction between self-assembled dentin matrix protein 1 and calcium phosphate nuclei in solution. Biochemistry 2005;44:16140–8. [PubMed: 16331974]
6. He G, George A. Dentin matrix protein 1 immobilized on type I collagen fibrils facilitates apatite deposition in vitro. J Biol Chem 2004;279:11649–56. [PubMed: 14699165]
7. Ling Y, Rios HF, Myers ER, Lu Y, Feng JQ, Boskey AL. DMP1 depletion decreases bone mineralization in vivo: an FTIR imaging analysis. J Bone Miner Res 2005;20:2169–77. [PubMed: 16294270]
8. Tartaix PH, Doulaverakis M, George A, Fisher LW, Butler WT, Qin C, Salih E, Tan M, Fujimoto Y, Spevak L, Boskey AL. In vitro effects of dentin matrix protein-1 on hydroxyapatite formation provide insights into in vivo functions. J Biol Chem 2004;279:18115–20. [PubMed: 14769788]
9. Yamazaki Y, Okazaki R, Shibata M, Hasegawa Y, Satoh K, Tajima T, Takeuchi Y, Fujita T, Nakahara K, Yamashita T, Fukumoto S. Increased circulatory level of biologically active full-length FGF-23 in patients with hypophosphatemic rickets/osteomalacia. J Clin Endocrinol Metab 2002;87:4957–60. [PubMed: 12414858]
10. Jonsson KB, Zahradnik R, Larsson T, White KE, Sugimoto T, Imanishi Y, Yamamoto T, Hampson G, Koshiyama H, Ljunggren O, Oba K, Yang IM, Miyauchi A, Econs MJ, Lavigne J, Juppner H. Fibroblast growth factor 23 in oncogenic osteomalacia and X-linked hypophosphatemia. N Engl J Med 2003;348:1656–63. [PubMed: 12711740]
11. Ogbureke KU, Fisher LW. Expression of SIBLINGs and their partner MMPs in salivary glands. J Dent Res 2004;83:664–70. [PubMed: 15329369]
12. Ogbureke KU, Fisher LW. Renal expression of SIBLING proteins and their partner matrix metalloproteinases (MMPs). Kidney Int 2005;68:155–66. [PubMed: 15954904]
13. Livak KJ, Schmittgen TD. Analysis of relative gene expression data using real-time quantitative PCR and the 2(-Delta Delta C(T)) Method. Methods 2001;25:402–8. [PubMed: 11846609]
14. Stamp TC, Baker LR. Recessive hypophosphataemic rickets, and possible aetiology of the ‘vitamin D-resistant’ syndrome. Arch Dis Child 1976;51:360–5. [PubMed: 180907]

15. Baker LR, Stamp TC. Autosomal recessive hypophosphataemia. Arch Dis Child 1989;64:1209. [PubMed: 2782942]

16. Kolek OI, Hines ER, Jones MD, LeSueur LK, Lipko MA, Kiela PR, Collins JF, Haussler MR, Ghishan FK. 1alpha, 25-Dihydroxyvitamin D3 upregulates FGF23 gene expression in bone: the final link in a renal-gastrointestinal-skeletal axis that controls phosphate transport. Am J Physiol Gastrointest Liver Physiol 2005;289:G1036–42. [PubMed: 16020653]

17. Foster BL, Nociti FH Jr, Swanson EC, Matsa-Dunn D, Berry JE, Cupp CJ, Zhang P, Somerman MJ. Regulation of cementoblast gene expression by inorganic phosphate in vitro. Calcif Tissue Int 2006;78:103–12. [PubMed: 16467974]

18. Qin C, Baba O, Butler WT. Post-translational modifications of sibling proteins and their roles in osteogenesis and dentinogenesis. Crit Rev Oral Biol Med 2004;15:126–36. [PubMed: 15187031]

19. Polisson RP, Martinez S, Khoury M, Harrell RM, Lyles KW, Friedman N, Harrelson JM, Reisner E, Drezner MK. Calcification of entheses associated with X-linked hypophosphatemic osteomalacia. N Engl J Med 1985;313:1–6. [PubMed: 4000222]

20. Hardy DC, Murphy WA, Siegel BA, Reid IR, Whyte MP. X-linked hypophosphatemia in adults: prevalence of skeletal radiographic and scintigraphic features. Radiology 1989;171:403–14. [PubMed: 2539609]

21. The HYP Consortium. A gene (PEX) with homologies to endopeptidases is mutated in patients with X-linked hypophosphatemic rickets. Nat Genet 1995;11:130–6. [PubMed: 7550339]

22. Narayanan K, Ramachandran A, Hao J, He G, Park KW, Cho M, George A. Dual functional roles of dentin matrix protein 1. Implications in biomineralization and gene transcription by activation of intracellular Ca2+ store. J Biol Chem 2003;278:17500–8. [PubMed: 12615915]

23. Qin C, D'Souza R, Feng JQ. Dentin matrix protein 1 (DMP1): new and important roles for biomineralization and phosphate homeostasis. J Dent Res 2007;86:1134–41. [PubMed: 18037646]

24. Narayanan K, Gajjeraman S, Ramachandran A, Hao J, George A. Dentin matrix protein 1 regulates dentin sialophosphoprotein gene transcription during early odontoblast differentiation. J Biol Chem 2006;281:19064–71. [PubMed: 16679514]

25. Yu X, Sabbagh Y, Davis SI, Demay MB, White KE. Genetic dissection of phosphate- and vitamin D-mediated regulation of circulating Fgf23 concentrations. Bone 2005;36:971–7. [PubMed: 15869926]

26. Ito M, Sakai Y, Furumoto M, Segawa H, Haito S, Yamanaka S, Nakamura R, Kuwahata M, Miyamoto K. Vitamin D and phosphate regulate fibroblast growth factor-23 in K-562 cells. Am J Physiol Endocrinol Metab 2005;288:E1101–9. [PubMed: 15671080]

27. Perwad F, Azam N, Zhang MY, Yamashita T, Tenenhouse HS, Portale AA. Dietary and serum phosphorus regulate fibroblast growth factor 23 expression and 1,25-dihydroxyvitamin D metabolism in mice. Endocrinology 2005;146:5358–64. [PubMed: 16123154]

28. Nishida Y, Taketani Y, Yamanaka-Okumura H, Imamura F, Taniguchi A, Sato T, Shuto E, Nashiki K, Arai H, Yamamoto H, Takeda E. Acute effect of oral phosphate loading on serum fibroblast growth factor 23 levels in healthy men. Kidney Int 2006;70:2141–7. [PubMed: 17063170]

29. Burnett SM, Gunawardene SC, Bringhurst FR, Juppner H, Lee H, Finkelstein JS. Regulation of C-terminal and intact FGF-23 by dietary phosphate in men and women. J Bone Miner Res 2006;21:1187–96. [PubMed: 16869716]

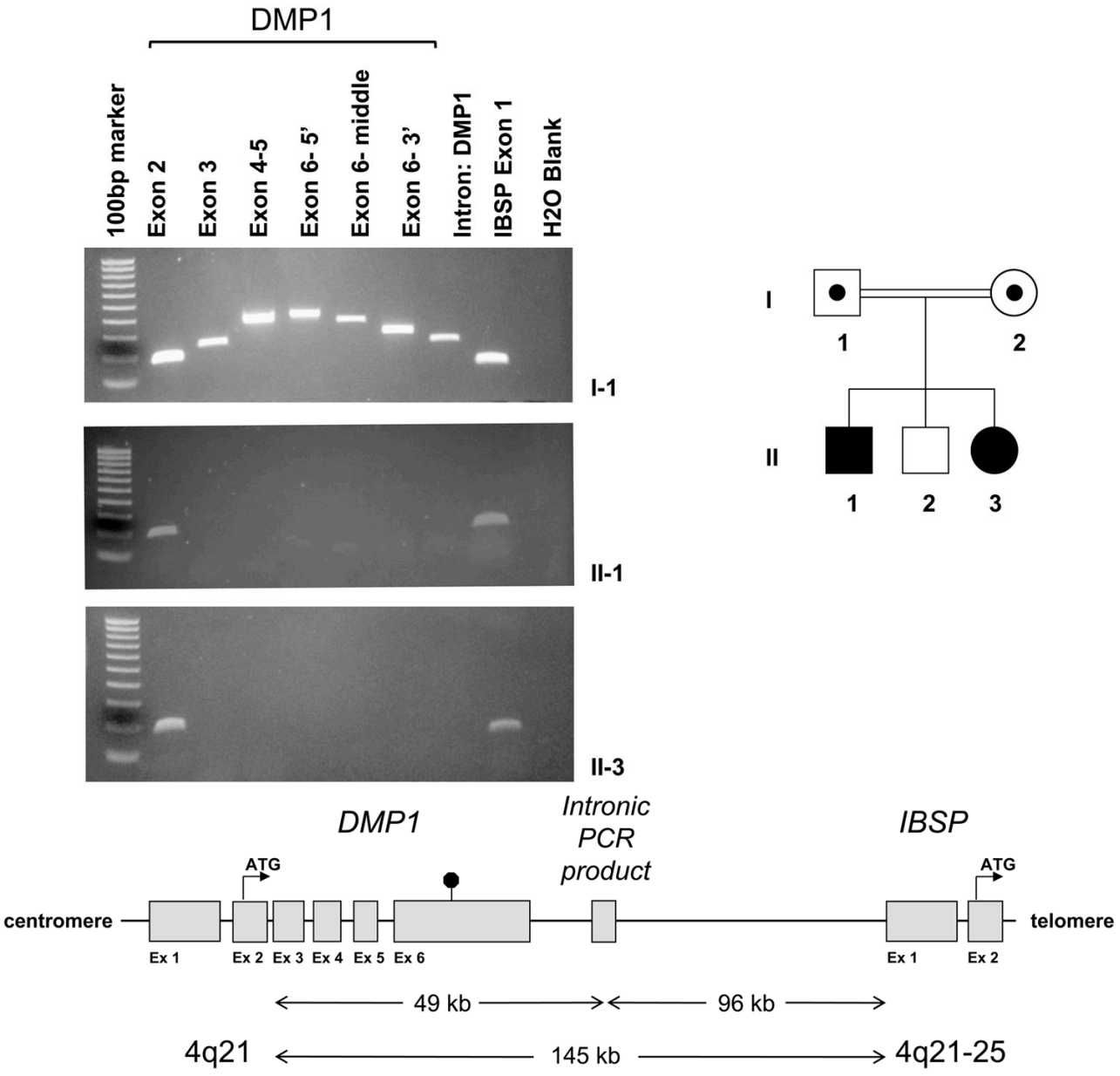

Figure 1. Novel ARHR *DMP1* mutation

A.) The PCR amplification of DMP1 exons, intergenic region, and IBSP from unaffected father (I-1) and the ARHR patients (II-1 affected brother and II-3 affected sister) revealed a large deletion in the patients. The family pedigree of individuals with recessive hypophosphatemia assessed in these studies is shown on the right. B.) A schematic of the deletion between DMP1 and IBSP in this kindred. The deletion is a minimum of 49 kb and a maximum of 145 kb (NCBI accession file NT_016354). The known gene exons are labeled as 'Ex.'

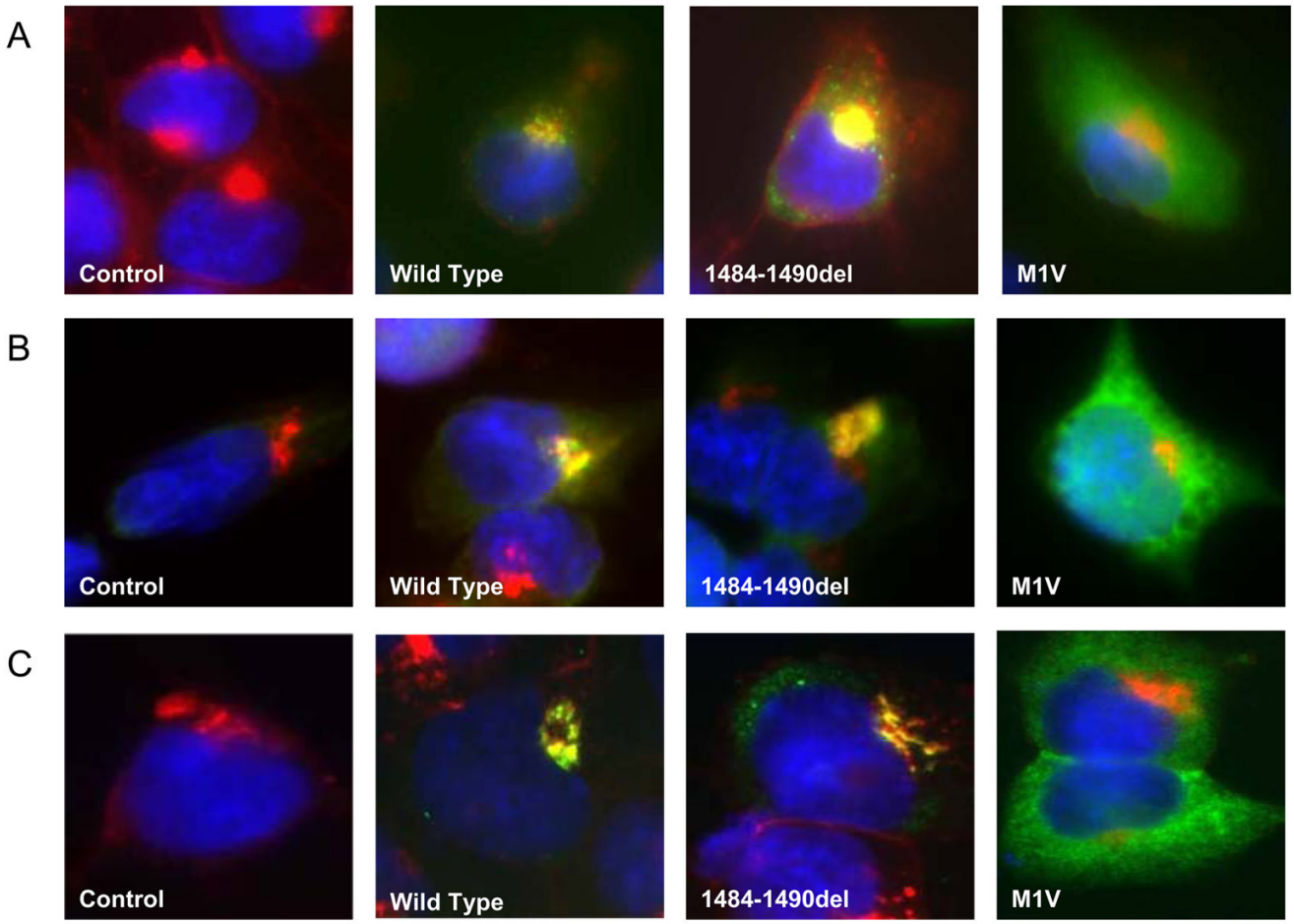

Figure 2. Cellular sorting of ARHR mutants

A.) UMR-106 cells were transfected with a wild type, 1484-1490del, or M1V DMP1 cDNAs. Immunofluorescent confocal analyses with anti-V5 showed that wild type DMP1 (green) was sorted to the TGN (red; red and green overlay is yellow), the M1V mutant (green) fills the cytoplasm and does not enter the TGN (red). Nuclei were stained with DAPI (blue). B.) The results in 2A were confirmed using an antibody specific to the TGN, TGN38 (red). C.) When DMP1 constructs were re-assessed lacking the C-terminal V5 tag using anti-human DMP1, the results are the same as in upper panels, demonstrating that the tag does not interfere with cellular processing

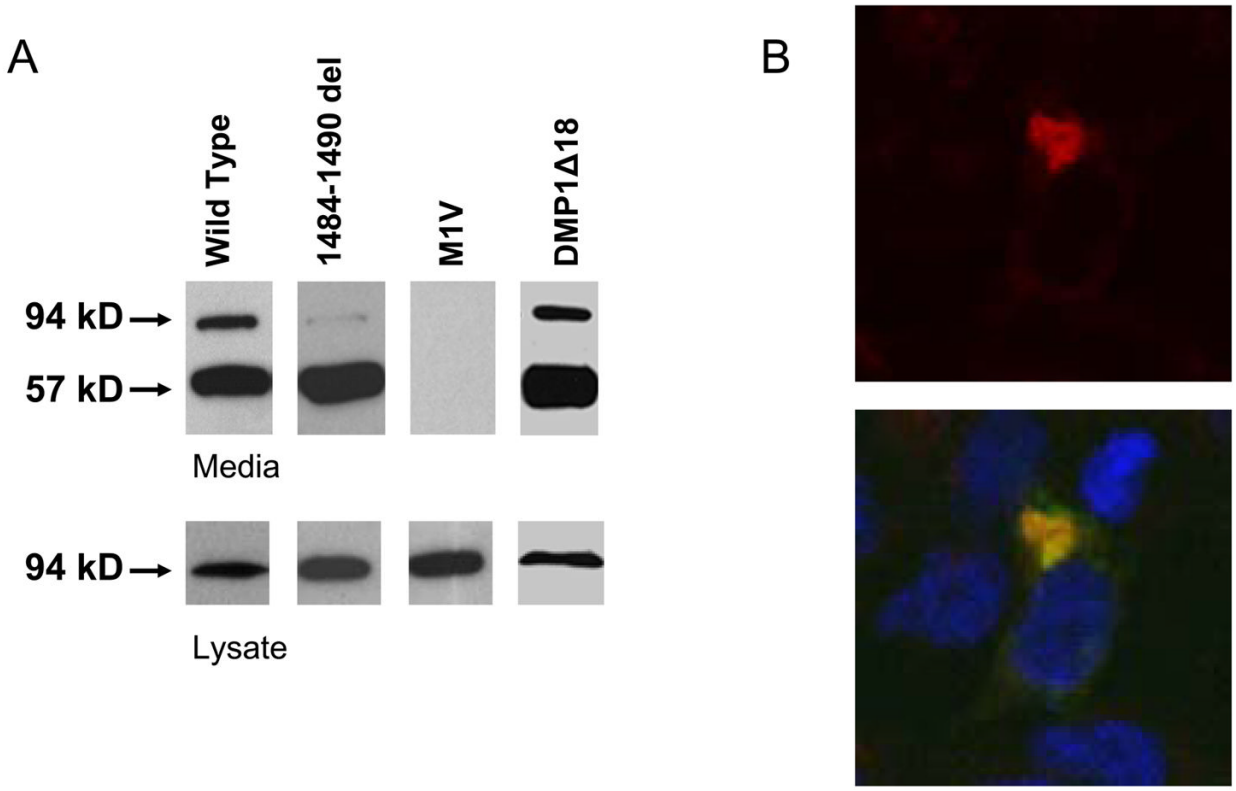

Figure 3. Analyses of conserved DMP1 C-terminal residues

A.) Transient transfection and Western analyses showed that the 94 and 57 kD species in conditioned media originating from the DMP1Δ18 plasmid (right lane), when compared to the 1484-1490del mutant, is processed and secreted similar to wild type DMP1 (left lane). The M1V mutant is not secreted into the media. B.) Immunofluorescent analysis of DMP1Δ18 in HEK293 cells with anti-V5 (green) showed co-localization with the TGN (red). The upper panel is the TGN, the lower panel is DMP1, nuclei (DAPI-blue), and the TGN merged.

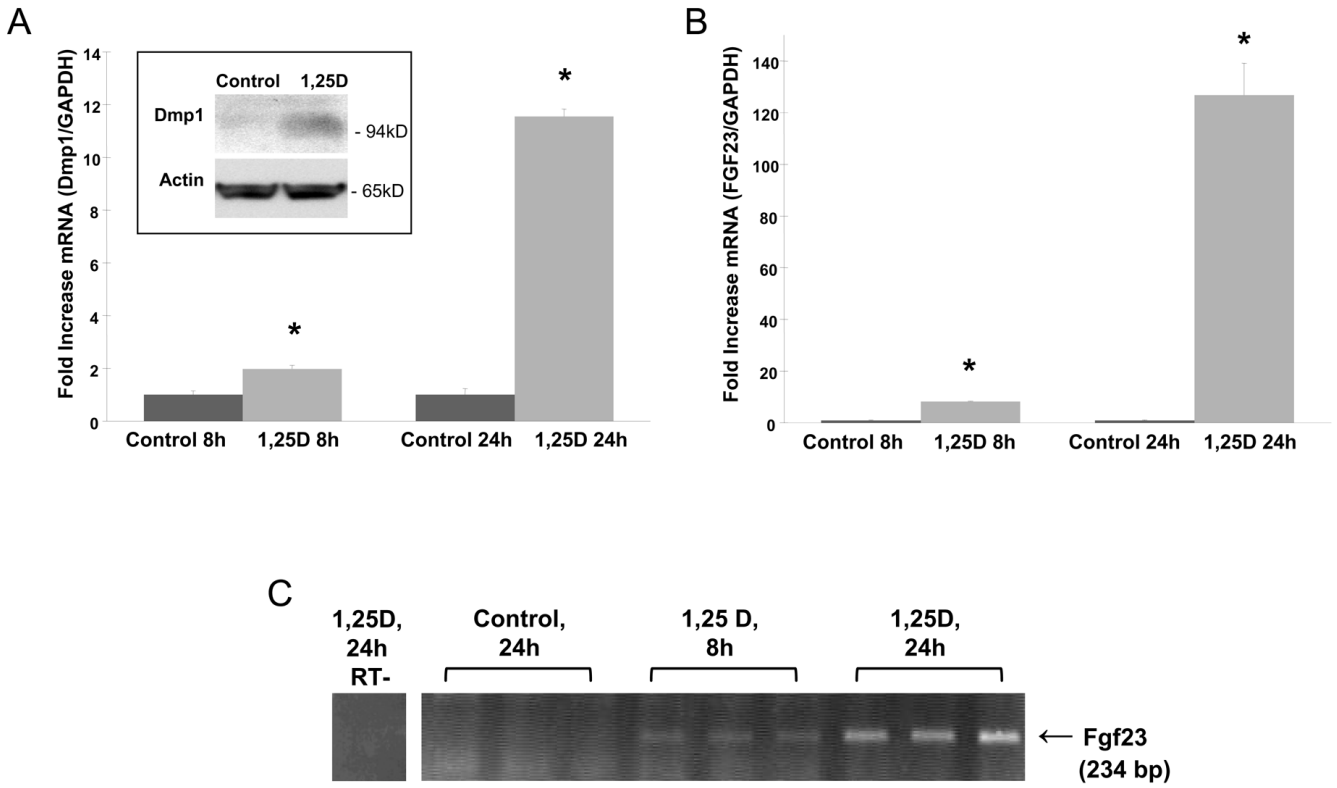

Figure 4. Vitamin D regulation of DMP1 in UMR-106 cells

UMR-106 cells were treated with either vehicle or 1×10^7 1,25$(OH)_2$ vitamin D (1,25D) for the times indicated. A.) DMP1 mRNA, assessed by qPCR was maximally elevated 12-fold at 24 hours when compared to vehicle-treated control cells (*; $P<0.05$). *Inset:* DMP1 protein was increased in the cell media as assessed by Western analysis when compared to vehicle-treated control cells at 24 h. Beta-actin from the lysates of the same cells is shown as control. FGF23 was also elevated with vitamin D treatment as determined by: B.) qPCR (*; $P<0.05$); and C.) qualitative RT-PCR with intron-spanning primers to rat FGF23.

Table 1

Serum biochemistries for the ARHR kindred.

Serum biochemistry	Patient II-1	Patient II-3
Serum phosphate (0.74–1.52 mmol/L)	0.87, 0.85	0.64
Serum Calcium (2.15–2.61 mmol/L)	2.43, 2.27, 2.41	2.17
PTH (1.4–6.4 pmol/L)	11.3, 5.4, 3.0	5.7
25-OH vitamin D (40–144 nmol/L)	92, 65, 57	NA
Creatinine (60–100 μmol/l)	76, 81	77

Normal range shown in parentheses (NA: *not available*)